A METAL-ON-SILICON DIFFERENTIAL CAPACITIVE SHEAR STRESS SENSOR

V. Chandrasekharan, J. Sells, J. Meloy, D.P. Arnold, and M. Sheplak
Interdisciplinary Microsystems Group, University of Florida, Gainesville, Florida, USA

ABSTRACT

The paper presents a direct, capacitive shear stress sensor with performance sufficient for time-resolved turbulence measurements. The device employs a bulk-micromachined, metal-plated, differential capacitive floating-element design. A simple, two-mask fabrication process is used with DRIE on an SOI wafer to form a tethered floating element structure with comb fingers for transduction. Experimental results indicate a linear sensitivity of $7.66\ mV/Pa$ up to the testing limit of $1.9\ Pa$ at a bias voltage of $10\ V$, and a bandwidth of $6.2\ kHz$. The sensor possesses a dynamic range $>102\ dB$ and a noise floor of $14.9\ \mu Pa/\sqrt{Hz}$ at $1\ kHz$, outperforming previously reported sensors by nearly two orders of magnitude in MDS.

KEYWORDS

Shear stress sensor, comb fingers, metal passivation, capacitive sensors

INTRODUCTION

Shear stress measurements are useful in a variety of applications, including fundamental study of turbulence, aerodynamic drag measurement, flow control feedback, and non-intrusive industrial flow measurement. Time-resolved shear stress measurements may also be used to validate computational turbulence models. For turbulence measurements, MEMS sensors scale favorably, offering the potential bandwidth and spatial resolution to capture the broad frequency spectrum and small-scale structures in turbulent flows [1]. Despite several research efforts, there is a lack of a fundamental measurement standard for wall shear stress measurements.

Floating element and thermal MEMS shear stress sensors have been developed previously for skin friction measurements in fluidic applications [1]. In thermal sensors, convective heat transfer between a heated element and the fluid is used to infer shear stress [2], which requires complex calibration [1]. Direct shear stress sensors measure the integrated shear force on a sensing surface using capacitive [3-5], optical [6], or piezoresistive [7] transduction schemes. However, previous efforts lacked practical viability due to drift, packaging complexity, poor performance in terms of noise floor, etc. [1]. The device presented here attempts to overcome some of these limitations via a) metallization of the electrically active silicon to eliminate charge accumulation and reduce drift, b) high transverse mechanical stiffness and a differential capacitive measurement scheme to reduce temperature sensitivity and cross-axis sensitivity, and c) hybrid packaging with the amplifier located in close proximity to the sensor, thus minimizing parasitics and electromagnetic interference.

FABRICATION AND PACKAGING

A floating element with interdigitated, asymmetric, capacitive comb fingers between the tethers, defines the shear stress sensor structure. The floating element is $2\ mm \times 2mm$ in area, $45\ \mu m$ thick, and supported by four tethers, $1000\ \mu m \times 23\ \mu m \times 45\ \mu m$. The comb fingers are each $170\ \mu m \times 5\ \mu m \times 45\ \mu m$. Asymmetric gaps ($3.5\ \mu m$ and $20\ \mu m$) between 116 interdigitated comb fingers form differential capacitors on either side of the sensor. Gaps between the stationary substrate and both the tethers and the non-fingered sides of the floating element provide additional capacitance for transduction and improve sensitivity. Figure 1 shows the schematic of the floating element sensor structure with comb fingers and also illustrates the process flow.

The sensor is fabricated using a simple and cost-effective 2-mask fabrication process. The process begins with a 4" diameter silicon on insulator (SOI) wafer with a $45\ \mu m$ thick, highly doped, p-type device layer on top of a $500\ \mu m$ thick float zone bulk substrate separated by a $2\ \mu m$ thick buried oxide (BOX) layer. The first mask pattern followed by deep reactive ion etching (DRIE) on the device layer defines the entire sensor structure, including bond pads for electrical contact. This step is followed by seedless electroplating of nickel on the highly conductive device layer. A second mask and a DRIE step are used to define the cavity underneath the floating

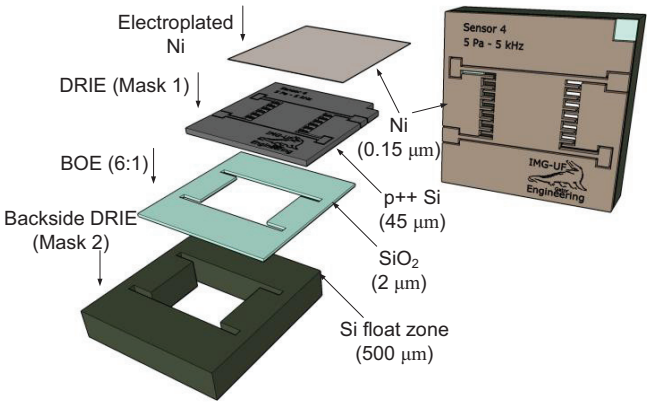

Figure 1 Schematic of sensor die indicating layers with front and backside DRIE and Ni plated sensor surface.

element. After wafer dicing, an isotropic buffered oxide wet etch (6:1 BOE) is used to etch the BOX, releasing individual sensor die. Supercritical dry in CO_2 follows the BOE etch to avoid stiction. Figure 2 shows the scanning electron microscopy (SEM) image of the asymmetric comb finger structure and uniformity of the electroplated Ni on a fractured comb finger cross-section.

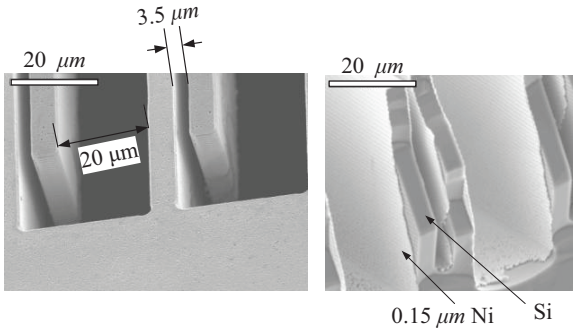

Figure 2 SEM images indicating the asymmetry in comb fingers (left) and electroplated Ni on the comb finger sidewalls (right).

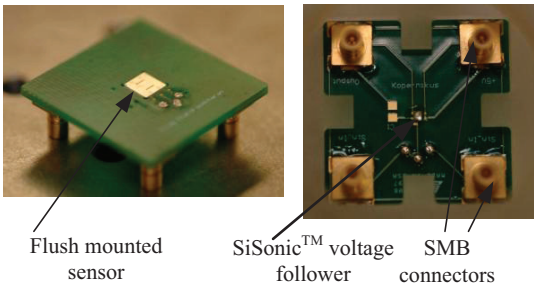

Figure 3 Sensor packaged on a (30 mm ×30 mm) PCB board, flush with the surface with voltage follower and electrical connections on backside of the PCB to minimize parasitics.

The individual sensor die $(5\,mm \times 5\,mm)$ are then packaged with epoxy (Dualbond 707) in a printed circuit board (PCB) with a recess to enable flush mounting of the sensor. Wire bonds connect the sensor to electrical contacts on the PCB (Figure 3). A SiSonic™ [8] voltage amplifier (unity gain) is used to read the differential output voltage (Figure 3). The PCB is later packaged in a Lucite plug for dynamic sensor calibration.

EXPERIMENTAL RESULTS

The sensor is characterized for shear stress and noise performance to estimate its sensitivity, dynamic range, frequency response, noise floor, and minimum detectable shear stress (MDS). Die-level impedance measurements are used to estimate the nominal sensor capacitance. The nominal single-ended capacitance, including parasitics, is $14\,pF$. Figure 4 shows an image of the sensor structure and the differential capacitance measurement scheme for post-packaged sensor characterization.

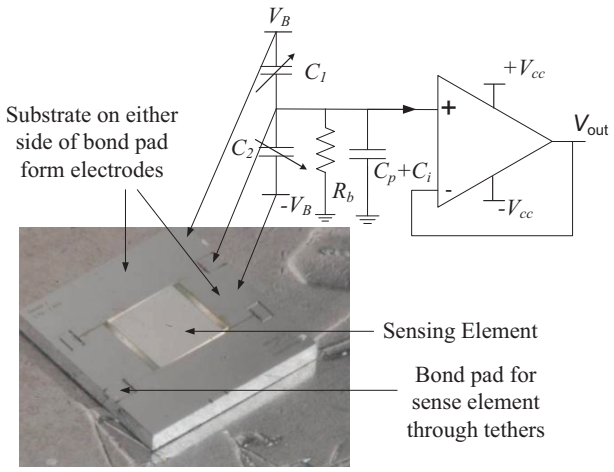

Figure 4 Schematic with optical image of sensor die (5 mm ×5 mm) indicating floating element, contact pads, and differential capacitance interface circuit.

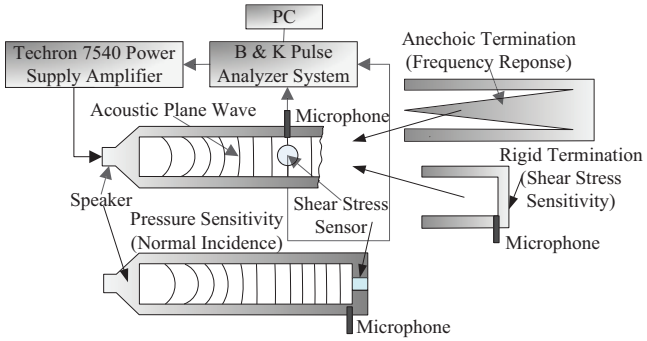

Figure 5 Schematic of the dynamic calibration setup in the PWT for measuring dynamic sensitivity, frequency response and pressure sensitivity.

Dynamic Characterization

The dynamic shear stress sensitivity and frequency response of the sensor are characterized by Stokes layer excitation, which uses acoustic plane waves in a duct providing a known sinusoidal shear stress input (τ_{in}) to the sensor [9]. Figure 5 shows the setup for sensor calibration in a plane wave tube (PWT). The PWT has a 1" × 1" duct cross section, which permits testing up to $6.7\,kHz$ (in air), beyond which higher order modes propagate. A BMS 4590P compression driver generates acoustic waves at one end of the PWT, and a reference microphone (B&K 4138, 1/8"), mounted appropriately (based on termination), measures p'. A B&K PULSE Multi-Analyzer System (Type 3109) serves as the microphone power supply, data acquisition unit, and signal generator for the compression driver. For all dynamic measurements the sensor is biased using differential dc bias voltages, $V_B = \pm 10\,V$. One complication for acoustic shear stress excitation is that both pressure and shear stresses are acting on the floating element. Although

designed to reject pressure fluctuations, the shear stress sensor has the propensity to respond to both, and these effects must be accounted for in the characterization.

For shear stress linearity characterization, the sensor is flush mounted in the PWT sidewall at a known distance from a rigid termination, which establishes a standing wave pattern [10]. Since shear stress is a function of the velocity gradient, the acoustic frequency ($1.128\ kHz$) is chosen such that sensor is located at a velocity maxima and pressure minima (quarter wavelength from termination). A reference microphone is located at the termination to measure the peak pressure (Figure 3). For testing, the peak sound pressure level (SPL) is increased from $80\ dB\left(\text{ref.}20\mu Pa\right)$ to $160\ dB$ in steps of $5\ dB$ at $f=1.128\ kHz$. The sensor exhibits a linear dynamic shear stress sensitivity of $7.66\ mV/Pa$ up to the testing limit of $\tau_{in}=1.9\ Pa$ (Figure 6). A second reference microphone monitors the pressure at the sensor location (same axial position along the PWT). The pressure acting on the sensor is consistently lower ($\approx 40\ dB$) than the peak pressure measured at the termination, confirming a position of minimal pressure.

For the frequency response measurement, the tube is fitted with an anechoic termination (30.7" long fiber glass wedge), allowing plane progressive waves within the duct. In this case, the reference microphone is at the same axial position as the sensor since both velocity and pressure maxima occur at the same location in a progressive wave. The frequency response function of the sensor is estimated using the expression,

$$H(f)=\left(\frac{V(f)}{\tau_{in}(f)}\right)\frac{\partial\bar{\tau}}{\partial\bar{V}}, \qquad (1)$$

where $V(f)$ is the sensor output voltage, $\tau_{in}(f)$ is the input shear stress, and $\partial\bar{\tau}/\partial\bar{V}$ is the inverse of the shear stress sensitivity estimated at $f=1.128\ kHz$. The frequency and the SPL are varied to maintain a constant magnitude of input shear stress, $|\tau_{in}|=0.5\ Pa$ (Figure 7). The results indicate the sensor has a response similar to the expected second order system response with an estimated resonance at $6.2\ kHz$. Although the shear stress sensitivity is used in Eq. (1), the sensor output voltage is a composite result of both pressure and shear inputs. Therefore, the $|H(f)|$ results are qualitative and their quantitative accuracy is a subject of further scrutiny. This leads to investigation of the sensor performance under direct dynamic pressure excitation. Furthermore, in a real application like a turbulent flow, the pressure forces can be roughly two orders of magnitude higher than the shear forces [11].

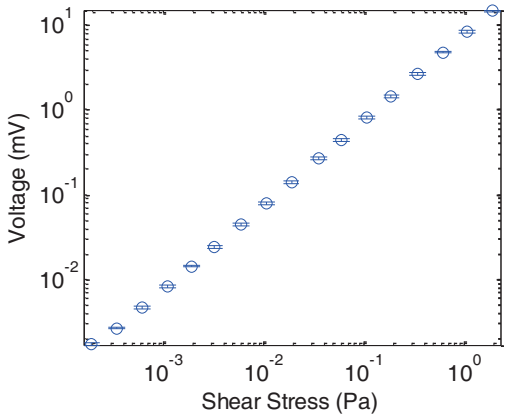

Figure 6 Linear dynamic shear stress sensitivity at V_B =10 V and f =1.128 kHz and the sensor placed quarter wavelength away from the rigid termination.

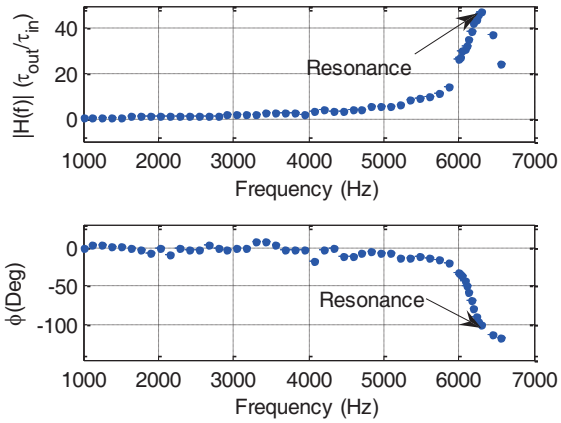

Figure 7 Frequency response of sensor at V_B = 10 V using $|\tau_{in}|$= 0.5 Pa as the reference input.

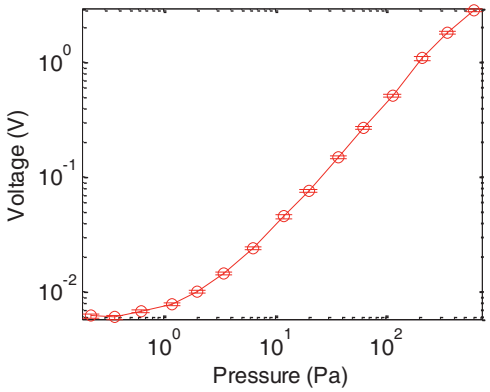

Figure 8 Sensor voltage output as a function of pressure using normal acoustic incidence in PWT at V_B = 10 V and f = 4.2 kHz.

For dynamic pressure sensitivity measurements, the PWT termination is replaced with the packaged sensor for normal acoustic incidence (Figure 5). The SPL is varied from $80\ dB$ to $150\ dB$ in steps of $5\ dB$ at $f=4.2\ kHz$. The measured pressure sensitivity of the sensor is

4.8 $\mu V/Pa$ (Figure 7). At low SPL the measured output is dominated by the noise floor of the data acquisition system. In comparison to S_{shear}, the pressure rejection is roughly 64 dB.

Noise Characterization

Noise measurements are conducted in a double Faraday cage on the packaged sensor to estimate the MDS. An SR 785 spectrum analyzer measures the output noise power spectral density (PSD) of the biased sensor. A Hanning window is applied with 75 % overlap to reduce spectral leakage. Measurements are performed both with and without the sensor to distinguish the sensor noise from that of the measurement system (spectrum analyzer and cabling). At $V_B = 10\ V$, the output referred noise PSD of the sensor is 114 $nV/\sqrt{Hz}$ at 1 kHz with 1 Hz bin. This is equivalent to an MDS of 14.9 $\mu Pa/\sqrt{Hz}$, which is the ratio of the electronic noise to the shear stress sensitivity.

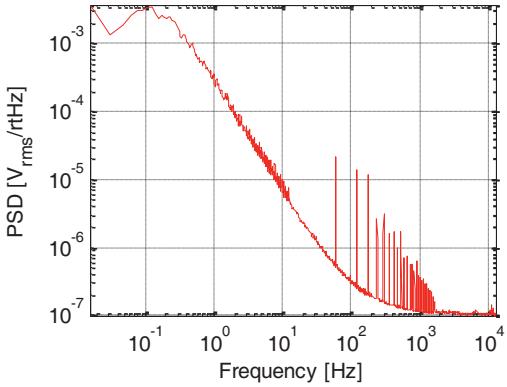

Figure 9 Measured output referred noise floor of the packaged sensor in $V_{rms}/\sqrt{Hz}$ at $V_B = 10\ V$.

*Table 1 Comparison of experimental results to previous work (*theoretically predicted).*

Shear Stress Sensor	Element Size (mm)	τ_w Range (Pa)	f_{max} (kHz)	Sensitivity (mV/Pa)
Present Work	2	1.9 – 14.9E-6	6.2	7.66
Zhe [5]	3.2	0.16 – 0.04	0.531*	337
Padmanabhan [6]	0.5	10 – 1.4E-3	16*	320
Schmidt [3]	0.5	13 – 0.01*	10*	0.47

CONCLUSIONS

The development of a micromachined differential capacitive shear stress sensor is presented. The asymmetric comb finger structure allows the use of a single material layer to define the sensor structure and bond pads for electrical contact. This also reduces fabrication complexity, enabling a simple, two-mask process. Potential drift issues are mitigated via direct electroplated Ni passivation layer on conductive Si. The sensor has a dynamic range of 1.9 Pa – 14.9 μPa or 102 dB, which is potentially even higher given that the output voltage is still linear at the highest measured shear stress of 1.9 Pa and the sensor design is for at least 5 Pa. A pressure rejection of 64 dB is achieved via structural design and the differential capacitance scheme. Table 1 compares this device with previous research efforts.

ACKNOWLEDGEMENTS

Financial support for this work is provided by NASA (NNX07AB27A) and Florida Center for Advanced Aeropropulsion (FCAAP).

REFERENCES

[1] J. W. Naughton and M. Sheplak, "Modern Development in Shear Stress Measurement," *Prog. Aero. Sci.,* vol. 38, pp. 515-570, 2002.

[2] C. Liu, J. B. Huang, Z. J. Zhu, F. K. Jiang, S. Tung, Y. C. Tai, and C. M. Ho, "Micromachined flow shear-stress sensor based on thermal transfer principles," *JMEMS,* vol. 8, pp. 90-99, Mar 1999.

[3] M. A. Schmidt, R. T. Howe, S.D.Senturia, and J. H. Haritonidis, "Design and Calibration of a Micromachined Floating-Element Shear-Stress Sensor," *TED,* vol. Ed-35, pp. 750-757, 1988.

[4] D. Hyman, T. Pan, E. Reshotko, and M. Mehregany, "Microfabricated shear stress sensors, Part 2: Testing and calibration," *AIAA J.,* vol. 37, pp. 73-78, Jan 1999.

[5] J. Zhe, V. Modi, and K. R. Farmer, "A microfabricated wall shear-stress sensor with capacitative sensing," *JMEMS,* vol. 14, pp. 167-175, Feb 2005.

[6] A. Padmanabhan, M. Sheplak, K. D. Breuer, and M. A.Schmidt, "Micromachined Sensors for Static and Dynamic Shear Stress Measurements in Aerodynamic Flows," *IEEE Trans. '97,* pp. 137-140, 1997.

[7] A. A. Barlian, S. J. Park, V. Mukundan, and B. L. Pruitt, "Design and characterization of microfabricated piezoresistive floating element-based shear stress sensors," *Sens. Act. A,* vol. 134, pp. 77-87, Feb 2007.

[8] P. V. Loeppert and S. B. Lee, "SiSonic™ - The first commercialized MEMS microphone," *Sens. and Act. Workshop*, Hilton Head, SC, 2006, pp. 27-30.

[9] M. Sheplak, A. Padmanabhan, M. A. Schmidt, and K. S. Breuer, "Dynamic Calibration of a Shear-Stress Sensor Using Stokes-Layer Excitation," *AIAA J.,* vol. 39, pp. 819-823, May 2001.

[10] D. T. Blackstock, "Fundamentals of physical acoustics," *Wiley Inc.,* New York, 2000, pp. 136.

[11] Z. W. Hu, C. L. Morfey, and N. D. Sandham, "Wall pressure and shear stress spectra from direct simulations of channel flow," *AIAA J.,* vol. 44, pp. 1541-1549, Jul 2006.

CONTACT

* M. Sheplak, tel: +1-352-392-3983; sheplak@ufl.edu